# Kharagpur Lecture 9
# Lyapunov Instability , Spectra , Fractals

1. Pendulum Lyapunov Spectrum by Rescaling
2. Systematics of the Gram-Schmidt Orthonormalization Algorithm
3. Lyapunov Spectra by Lagrange Multipliers
4. Lyapunov Spectra by Linearization ( "tangent space" )
5. Spectra for Various Mesoscopic Systems
6. Dimensionality Loss in Nonequilibrium Systems
7. Revisiting the Nonequilibrium Baker Map with Poincaré

William G. Hoover

Ruby Valley Nevada

December 2016

## 1. Lyapunov Instability , Spectra , Fractals

Lyapunov instability implies *exponential* growth of $\delta \rightarrow \delta(0)\exp[+\lambda t]$ .
Areas and Volumes in phase space grow exponentially too: $\exp[+\Sigma\lambda t]$ .
The growth rate of an area is $\lambda_1 + \lambda_2$ and of a volume $\lambda_1 + \lambda_2 + \lambda_3$ .
Evidently in a 2N-dimensional phase space there are 2N exponents .
In Hamiltonian mechanics the sum of all these exponents is zero !
This follows from Liouville's Theorem → $(df/dt) = 0$ .

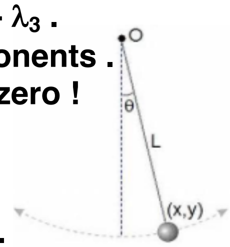


Conservation of probability $(f\oplus)$ gives also :

$d\ln(f\oplus)/dt = (d\ln f/dt) + (d\ln \oplus/dt) = 0 \rightarrow (d\ln \oplus/dt) = \Sigma\lambda = 0$ .

Liouville's Theorem shows that $(f\oplus)$ and f and $\oplus$ are *all* conserved in Hamiltonian flows . This is true *instantaneously* and time-averaged .

In order to understand this better let us illustrate all of these ideas with the springy pendulum problem , where $\mathcal{H} = (p^2/2) + y + 2(L - 1)^2$ .

## 1. Lyapunov Instability , $\mathcal{H} = (p^2/2) + y + 2(r - 1)^2$

There are four motion equations:

$$(dx/dt) = p_x \ ; \ (dy/dt) = p_y \ ;$$

$$(dp_x/dt) = -4(x/r)(r-1) \ ; \ (dp_y/dt) = -4(y/r)(r-1) - 1 \ .$$

Let us solve *five* copies all together , separated in four orthogonal phase-space directions by an "infinitesimal delta = 0.000001" :

```
x1 = xr + delta ; y1 = yr ; px1 = pxr ; py1 = pyr
x2 = xr ; y2 = yr + delta ; px2 = pxr ; py2 = pyr
x3 = xr ; y3 = yr ; px3 = pxr + delta ; py3 = pyr
x4 = xr ; y4 = yr ; px4 = pxr ; py4 = pyr + delta
 [ Reference { xr,yr,pxr,pyr } and four satellites ]
```

Provided that we can keep the solutions orthogonal the four offsets can be rescaled at every timestep to determine the four { $\lambda_i$ } . We have seen that rescaling the reference-to-satellite distance → $\lambda_1$ .

## 1. Lyapunov Instability for $\mathcal{H} = (p^2/2) + y + (\kappa/2)(r - 1)^2$

At the end of the first timestep we get 5 new values of { $x,y,p_x,p_y$ } .

$\delta_1 = (r_1 - r_r) \rightarrow \delta$ which gives us the instantaneous $\lambda_1$ . This is the *logarithm* of the scale factor ( $\delta / \delta_1$ ) divided by `-dt` . Just as is usual we will get a sum of these instantaneous { $\lambda_1$ } to get < $\lambda_1$ > . Next we force $\delta_2 = (r_2 - r_r)$ to remain orthogonal to $\delta_1$ . To do this we remove the projection of $\delta_2$ in the direction of $\delta_1$ :

$$\delta_2 = \delta_2 - \delta_1 (\delta_1 \bullet \delta_2)/(|\delta_1| \, |\delta_2|) \ .$$

We repeat this orthogonalization step for $\delta_3$ and $\delta_4$ . Rescaling $\delta_2$ gives the instantaneous $\lambda_2$ . Next force $\delta_3 = (r_3 - r_r)$ and $\delta_4$ to remain orthogonal to $\delta_2$ . Rescaling $\delta_3$ gives $\lambda_3$ . Finally we remove the projection of $\delta_4$ parallel to $\delta_3$ and rescale $\delta_4$ to get the fourth and last of the instantaneous Lyapunov exponents $\lambda_4$ .

## 2. Lyapunov Instability for $\mathcal{H} = (p^2/2) + y + (\kappa/2)(r - 1)^2$

Let us summarize the procedure giving the four exponents :

1. Integrate the 20 equations with RK4 to get $\{ \delta_1, \delta_2, \delta_3, \delta_4 \}$ .
2. Rescale $\delta_1$ to get $\lambda_1$ .
3. Remove the projections of $\{ \delta_2, \delta_3, \delta_4 \}$ parallel to $\delta_1$ .
4. Rescale $\delta_2$ to get $\lambda_2$ .
5. Remove the projections of $\{ \delta_3, \delta_4 \}$ parallel to $\delta_2$ .
6. Rescale $\delta_3$ to get $\lambda_3$ .
7. Remove the projection of $\{ \delta_4 \}$ parallel to $\delta_3$ .
8. Rescale $\delta_4$ to get $\lambda_4$ .

This 8-step procedure is followed for every timestep . It is called "Gram-Schmidt" orthonormalization . With N equations the number of multiplies is of order $N^4$ . The N $\delta$ vectors have $O(N^2)$ dot products which are calculated O(N) times with each dot product requiring N multiplies .

## Lyapunov Instability for $\mathcal{H} = (p^2/2) + y + (\kappa/2)(r - 1)^2$

Some observations from the springy pendulum problem :

1. The four exponents sum to zero ( Liouville )
2. Soon $\lambda_1(t) = -\lambda_4(t)$ and $\lambda_2(t) = -\lambda_3(t)$ ( "pairing" ) *
3. Knowing this we need only to measure $\langle \lambda_1(t) \rangle = \lambda_1$
4. We could just as easily use polar coordinates →

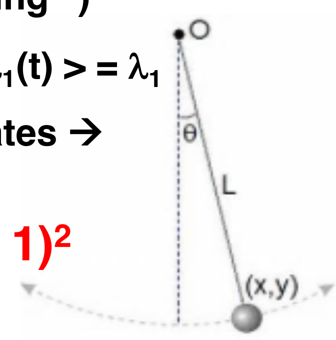


$$\mathcal{H} = (p^2/2) - r\cos(\theta) + (\kappa/2)(r - 1)^2$$

* Is this obvious ?

## Lyapunov Instability for $\mathcal{H} = (p^2/2) - r\cos(\theta) + (\kappa/2)(r-1)^2$

With the pendulum horizontal and the motion radial with $\mathcal{H} = 1$ .

We use the Lagrangian $[ (dr/dt)^2 + (rd\theta/dt)^2 ]/2$ to rewrite $( p^2/2 )$ :

$p_r = (dr/dt)$ and $p_\theta = r^2(d\theta/dt)$ so that $( p^2/2 ) = [ p_r^2 + (p_\theta^2/r^2) ]/2$

In polar coordinates with $\kappa = 4$ the equations of motion are :

$$( dr/dt ) = p_r \; ; \; ( dp_r/dt ) = ( p_\theta^2/r^3 ) - 4(r-1) - \cos(\theta)$$

$$( d\theta/dt ) = ( p_\theta/r^2 ) \; ; \; ( dp_\theta/dt ) = - r\sin(\theta)$$

Let us compare the first one million iterations

using dt = 0.001 and both coordinate systems .

## Lyapunov Instability for Polar and Cartesian Coordinates

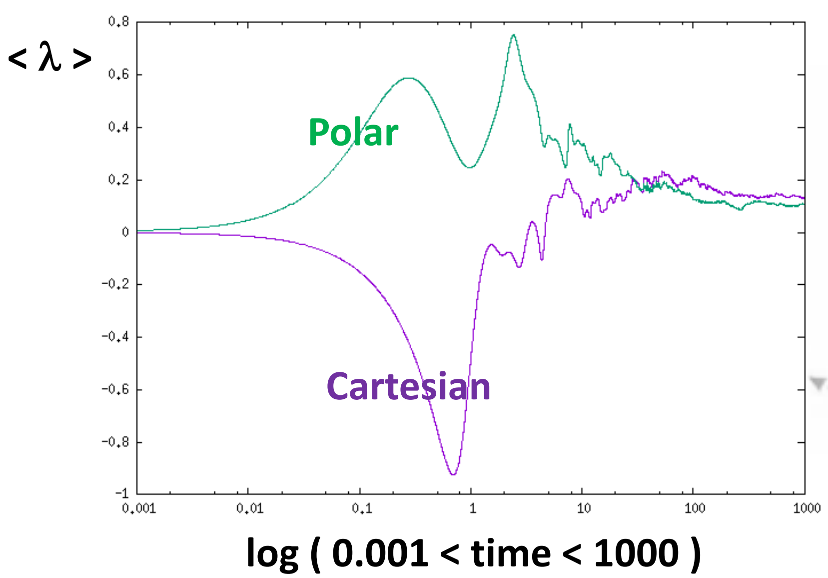


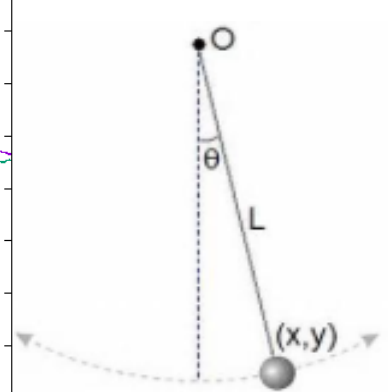

## Lyapunov Instability for Polar and Cartesian Coordinates*

In either Cartesian or Polar coordinates the time-reversibility of the motion equations gives "pairing" with

$$P( +\lambda_1 ) = P( -\lambda_4 ) \text{ and}$$
$$P( +\lambda_2 ) = P( -\lambda_3 ) .$$

The distributions depend on the coordinate system .

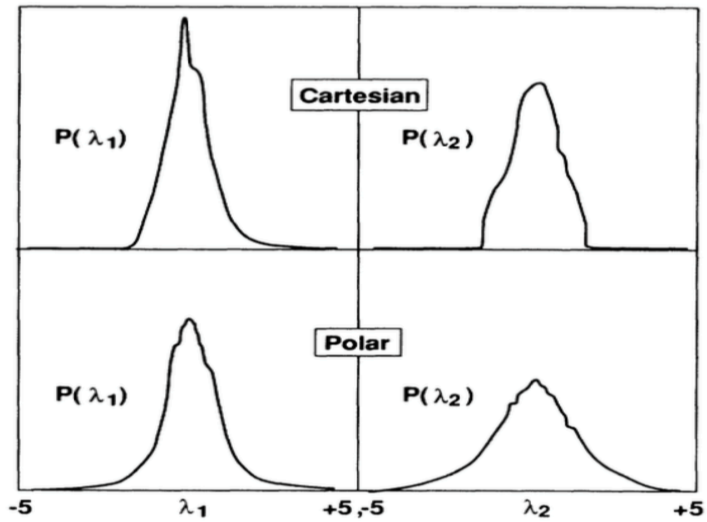


* For more details see *Time Reversibility, Computer Simulation, Algorithms, Chaos* (2012 ) page 31 .

## 3. Calculation of Lyapunov Spectra by Lagrange Multipliers

Let us detail the calculation of a single Lyapunov exponent $\lambda_1$ using a Lagrange multiplier . As before we have a "reference" trajectory and a "satellite" trajectory constrained to remain at a fixed distance $\delta$ from the reference .

[ 1 ] Solve the reference : $(dx_r /dt) = f(x_r)$ with RK4 or RK5 .
[ 2 ] Solve constrained satellite : $(dx_s /dt) = f(x_s) - \lambda(x_s - x_r)$

The multiplier $\lambda$ enforces the constraint that $| x_s - x_r | = \delta$ .

$$(x_s - x_r)[ f( x_s ) - \lambda(x_s - x_r) - f( x_r ) ] = 0 \rightarrow$$

$$(x_s - x_r)[ f( x_s ) - f( x_r ) ] / (x_s - x_r)^2 = \lambda$$

As an amazing fringe benefit the Lagrange Multiplier *is* $\lambda_1$ !

## 4. Calculation of Lyapunov Spectra in "tangent space"

$(dx/dt) = p_x$ ; $(dy/dt) = p_y$ ;
$(dp_x/dt) = -4(x/r)(r-1)$ ; $(dp_y/dt) = -4(y/r)(r-1) - 1$ . ( Gravity )

**To begin , *Linearize* the Cartesian motion equations in terms of**

**The *infinitesimal* tangent-space vector $(\delta x, \delta y, \delta p_x, \delta p_y)$ :**

$d\delta x/dt = \delta p_x$ and $d\delta y/dt = \delta p_y$

$d\delta p_x/dt = -4\delta x[1-(1/r)] - 4(x^2\delta x/r^3) - 4(xy\delta y/r^3)$

$d\delta p_y/dt = -4\delta y[1-(1/r)] - 4(y^2\delta y/r^3) - 4(xy\delta x/r^3)$

**Arbitrarily choose $\delta$ to be a unit vector : $|(\delta x, \delta y, \delta p_x, \delta p_y)| = 1$ .**

**We solve the four differential equations for the rotation of $\delta$ .**

## 4. Calculation of Lyapunov Spectra in "tangent space"

**[ Calculation is divided into ten batches in order to verify convergence ]**

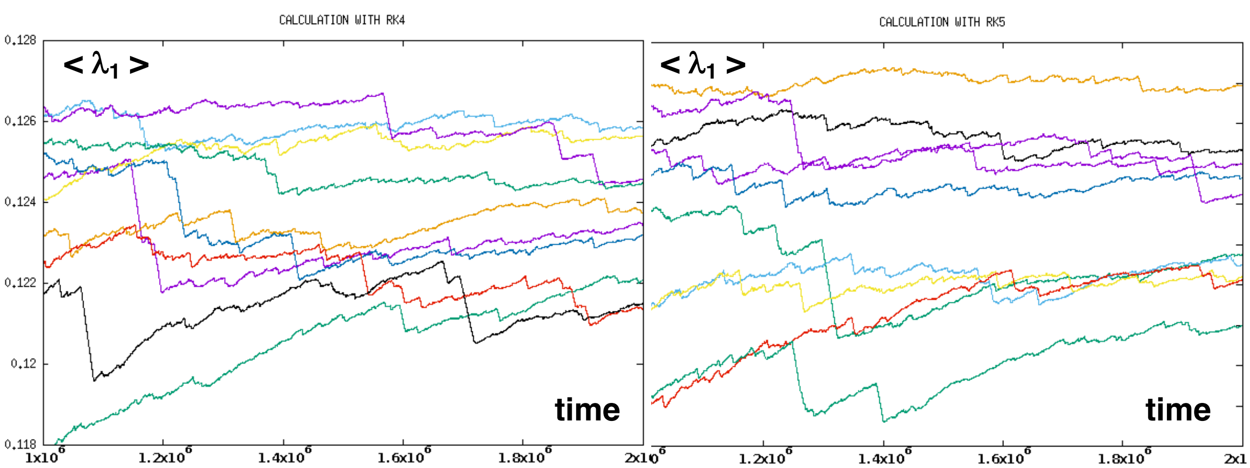


**Evidently the RK4 and RK5 { $0.124 = \lambda = \lambda_1$ } agree with our previous work .**

## Springy Pendulum Lyapunov Spectrum *via* Three Methods

**Lyapunov spectra describe many-dimensional phase-space deformation as well as the location of instabilities and bifurcations in dynamical systems. Consistent results can be obtained using Rescaling, Lagrange Multipliers, or Tangent-space algorithms . We studied an example problem involving the inelastic collision of two balls previously , finding the most important particles forward and back →**

## 1-4. Springy Pendulum Lyapunov Spectrum *via* Three Methods*

**Lyapunov spectra describe many-dimensional phase-space deformation in large or small-scale dynamical systems :**

**Here is the mesoscopic inelastic collision with Forward at left, Backward at right .**

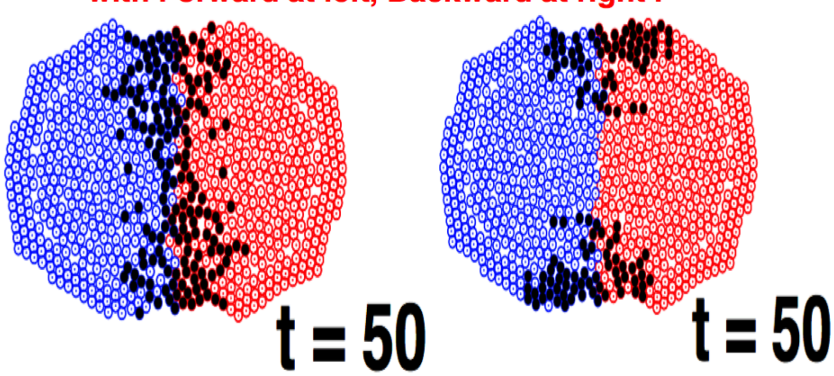


*** For this problem we developed a hybrid algorithm in which the reference trajectory is bit-reversible while fourth-order Runge-Kutta computation propagates the satellite trajectory ( or trajectories ) .**

# 2 – 4 . Applications of the three different methods for determining Lyapunov spectra

0. Gram-Schmidt Orthonormalization is Essential
1. Simple Numerical Rescaling at Every Step
2. Lyapunov Spectra by Lagrange Multipliers
3. Lyapunov Spectra by Linearization ( tangent space )

## 2 - 4. Systematics of the Gram-Schmidt Orthonormalization Algorithm

**Here are the steps to be carried out at the end of each timestep :**

| | |
|---|---|
| $\delta_1 \cdot \delta_1 \rightarrow \delta_1, \lambda_1$ | **Rescale the first vector, getting** $\delta_1, \lambda_1$ |
| $\delta_1 \cdot \delta_J \rightarrow \delta_J$ for $J > 1$ | **Remove projections on** $\delta_1$ |
| $\delta_2 \cdot \delta_2 \rightarrow \delta_2, \lambda_2$ | **Rescale the second vector, getting** $\delta_2, \lambda_2$ |
| $\delta_2 \cdot \delta_J \rightarrow \delta_J$ for $J > 2$ | **Remove projections on** $\delta_2$ |
| • • • | • • • |
| $\delta_N \cdot \delta_N \rightarrow \delta_N, \lambda_N$ | **Repeat until the whole spectrum results** |
| | **[ This can be done at every timestep . ]** |

Next :

Applications of the three methods for determining Lyapunov spectra

## 5. Equilibrium Spectra Resemble Solid-State Debye Spectra

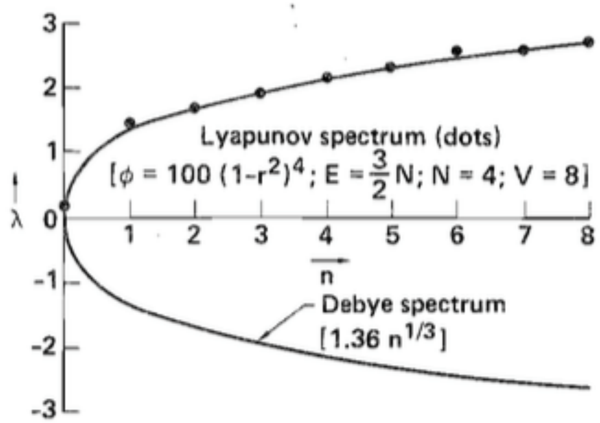


**Journal of Chemical Physics 87,** 6665-6670 **( 1987 ) .**

**Spectrum for four fluid particles in three space dimensions .**
**There are 24 exponents including 8 zeroes, 8 > 0 , and 8 < 0 .**
**Why are there 8 zeroes ?  Note that the exponents are paired .**

## 5. Here are Four Small-System Equilibrium Spectra in 2D and 3D*

**Periodic Boundaries**

**Short-Ranged Repulsive Forces**

**+/- Symmetry for the exponents'**

**Zeroes { D for r , D for p , E and t }**

**No zero exponents are shown .**

**Instantaneous Pairing is Typical .**

**Shear flows are *all laminar* with**

**Reynolds' Number *circa* 50 .**

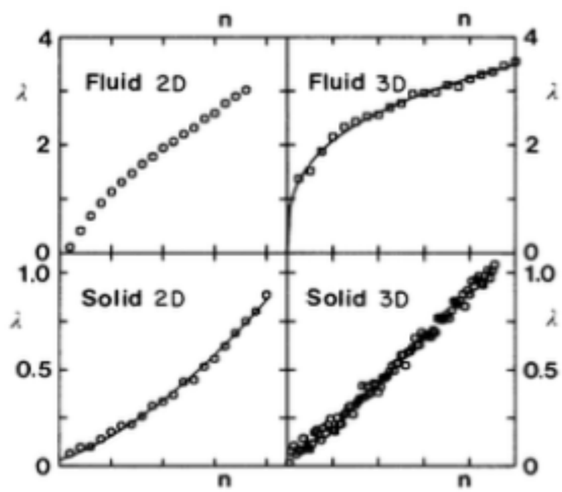


*** From Posch and Hoover, Physical Review A 39,** 2175-2188 **(1989) .**

## 6. Nonequilibrium Shear Flow Driven by Moving Boundaries

Notice that $P_{xy}$ is negative ( so that $\eta$ is positive )

$\lambda_1 = 8.7$

$\lambda_{69} = -43$

$\phi(r < 1) = 100(1 - r^2)^4$

Boundary mass = 1 and the horizontal temperature is unity

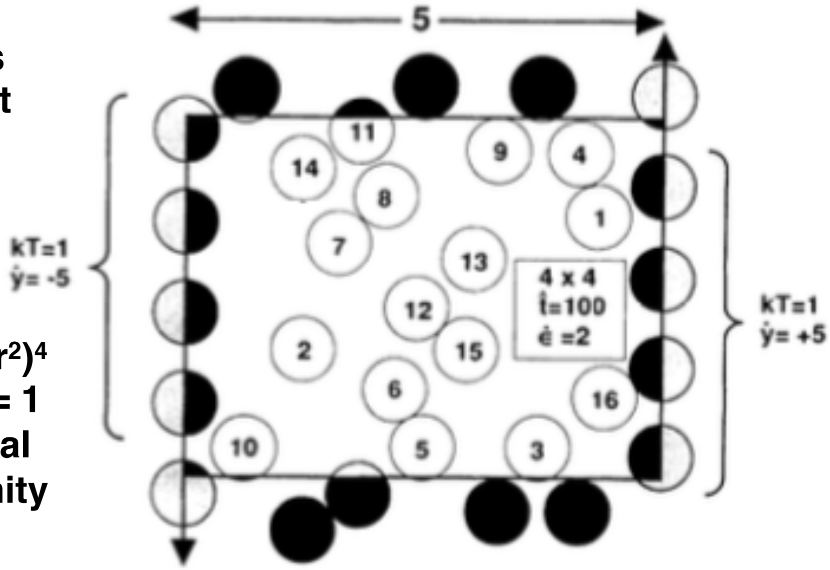


## 6. More Shear Flows Driven by Moving Boundaries

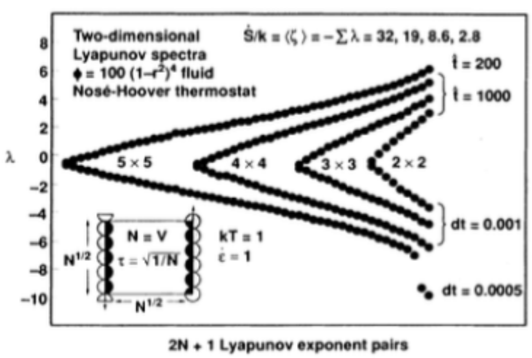


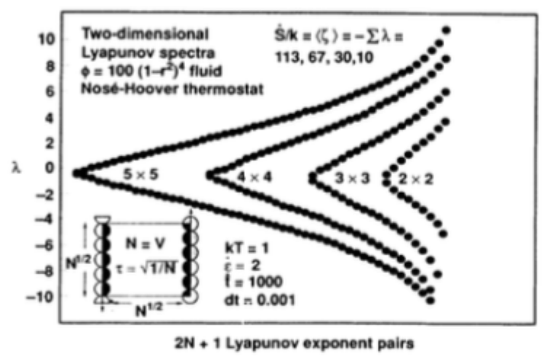


There is a *negative* shift of exponents, particularly the last few .
The sum of exponents changes sign between 63 and 64 terms .
This means there is a strange attractor with dimension 63.91 .

**Similar in 3D so that the dimensionality reduction is relatively small**

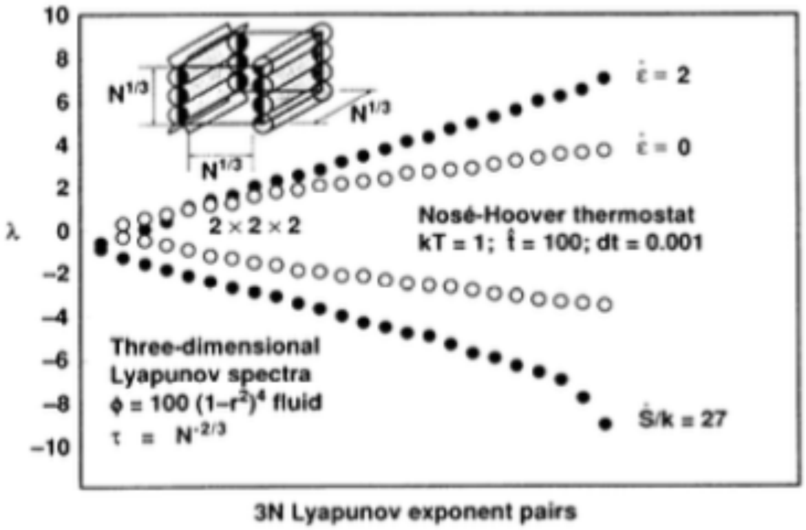


* Posch and Hoover, Physical Review A 39, 2175-2188 ( 1989 )

## 6. Spectra Bear a Resemblance to Solid-State Debye Spectra But That Interesting Shift Occurs Away from Equilibrium ! 1987 Conference Talk , Santa Trada Italy , Posch + Hoover

Here the potential is the repulsive part of the Lennard-Jones potential with $\rho = 0.5$ and $T = 1.0$ . There are 32 particles and 192 Lyapunov exponents . A field $F_e = 3$ drives half of the particles to the right and half to the left . An Amazing Observation is that the sum of all the exponents is negative , indicating that the phase volume is zero ! Temperature is kept fixed by using Gauss' Thermostat :

$\{ dp/dt = F - \zeta p \}$ ; $\zeta = - ( d\Phi/dt )/2K$ .

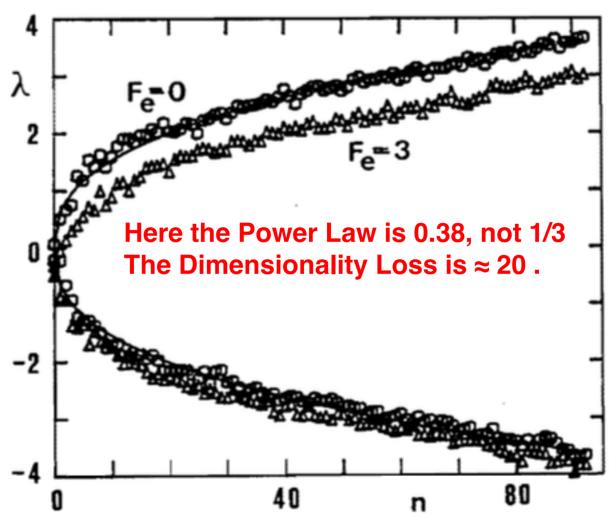

## The Idea of Heat Reservoirs Driving Nonequilibrium Systems as in Ashurst's Thesis led to an explanation of Irreversibility From Time-Reversible Nonequilibrium Molecular Dynamics .

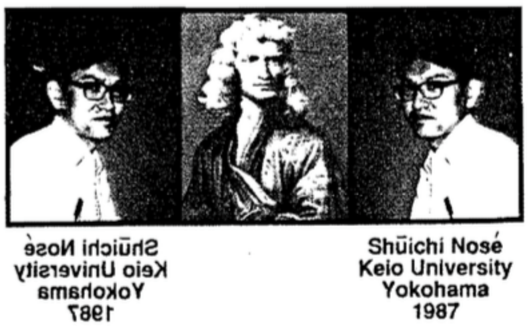


FIGURE 3
Schematic illustration of a far-from-equilibrium Newtonian bulk region driven by two reversible Nosé-Hoover heat revervoirs.

1987 Conference Talk at Monterey California . Work by Bill Hoover , Bill Moran, Brad Holian , Harald Posch . The stability of the simulation provides a mechanical proof of Thermodynamics' $2^{nd}$ Law .

## Thermal Heat Reservoirs *via* Gauss' Principle of Least Constraint ; Disssipation, Chaos, and Phase-Space Dimensionality Loss in One-Dimensional Chains*

The Heat Conductivity of a Harmonic chain diverges because the transport is ballistic . We decided to see what happens if a periodic chain is divided into two parts , each thermostated Into two parts, one cold and one hot , using Gaussian thermostat variables $\zeta$ and additional Lagrange multipliers $\eta$ , to constrain $\Sigma$ q , $\Sigma$ p , $\Sigma$ $p^2$ so that the equations of motion are :

$$\{ (dq/dt) = p \ ; \ (dp/dt) = F_{\mathcal{H}} - \zeta p - \eta \ ; \ \zeta = \Sigma F_{\mathcal{H}} p / \Sigma p^2 \ ; \ \eta = \Sigma F_{\mathcal{H}} / \Sigma 1 \}$$

A six-particle chain with both kinetic temperatures T = 2 is a chaotic Hamiltonian system . But partitioning the kinetic energy unequally , from ( 1.9,0.1 ) to ( 1.1,0.9 ) gives spectra corresponding to dissipative limit cycles ( no chaos ) . An eight-particle chain behaves differently , with a ( chaotic ) spectrum for temperature differences up to $\Delta K$ = 1.4 .

W G Hoover, H A Posch, and L W Campbell, Chaos 3, 325-332 ( 1993 ) .

## Thermal Heat Reservoirs *via* Gauss' Principle of Least Constraint ; Dissipation, Chaos, and Phase-Space Dimensionality Loss in One-Dimensional Chains*

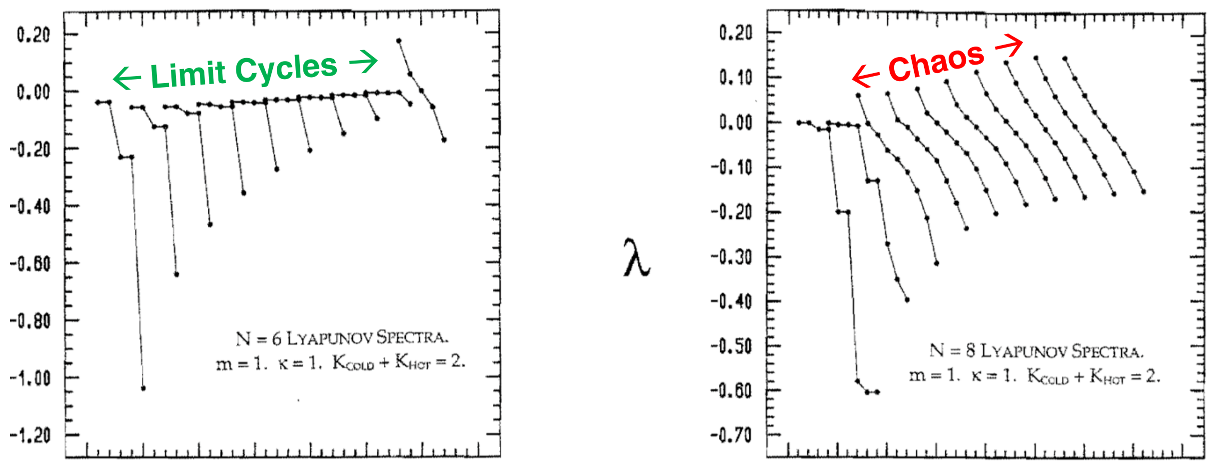


**6. Stationary States from HOT + COLD Harmonic Chains – a six or eight-particle chain is enough for chaos . Of the 2N Lyapunov exponents seven necessarily vanish , those representing the displacements , momenta , and kinetic energies of both regions plus motion in the trajectory direction .**

| $K_C$ | $K_H$ | $\Delta D(6)$ | $\Delta D(8)$ | $\dot{S}/k(6)$ | $\dot{S}/k(8)$ | $\lambda_1(6)$ | $\lambda_1(8)$ |
|---|---|---|---|---|---|---|---|
| 1.0 | 1.0 | 0.0 | 0.0 | 0.0 | 0.0 | 0.174 | 0.152 |
| 0.9 | 1.1 | 5.0 | 0.15 | 0.22 | $0.04_6$ | 0.00 | 0.152 |
| 0.8 | 1.2 | 5.0 | $0.5_8$ | 0.45 | 0.18 | 0.00 | 0.14 |
| 0.7 | 1.3 | 5.0 | $1.2_2$ | 0.70 | 0.39 | 0.00 | 0.118 |
| 0.6 | 1.4 | 5.0 | $2.1_7$ | 0.97 | 0.64 | 0.00 | 0.096 |
| 0.5 | 1.5 | 5.0 | $3.2_5$ | 1.29 | 0.92 | 0.00 | 0.078 |
| 0.4 | 1.6 | 5.0 | $4.3_4$ | 1.67 | 1.27 | 0.00 | 0.067 |
| 0.3 | 1.7 | 5.0 | 5.3 | 2.20 | 1.76 | 0.00 | 0.063 |
| 0.2 | 1.8 | 5.0 | 8.0 | 3.01 | 2.56 | 0.00 | 0.000 |
| 0.1 | 1.9 | 5.0 | 9.0 | 4.72 | 4.43 | 0.00 | 0.000 |

## Thermal Heat Reservoirs *via* Gauss' Principle of Least Constraint; Disssipation , Chaos , and Phase-Space Dimensionality Loss in One-Dimensional Chains*

**The harmonic model requires relatively intricate programming in order to maintain the six constraints ( center-of-mass position and momentum and temperature for both halves of the problem ) . There is an additional zero exponent corresponding to an offset in the direction of the trajectory motion . The $\phi^4$ model is considerably easier to implement and provides dimensionality losses with robust chaos .**

**Although Hamiltonian chaos is fascinating , with its mixture of chaotic and regular solutions , thermostated systems which avoid that complexity are certainly a more desirable approach to understanding nonequilibrium stationary states . The flow from an unstable repellor to a chaotic fractal attractor is far simpler than Hamiltonian chaos . The repellor/attractor structure can be seen in the smallest one-body models with either impulsive or continuous forces or even with two-dimensional maps .**

*** Hoover , Posch , and Campbell , Chaos 3 ,** 325-332 **( 1993 )**

## The Reversibility of the Equations of Motion Implies the Presence of Attractor + Repellor Pairs of Fractal Objects

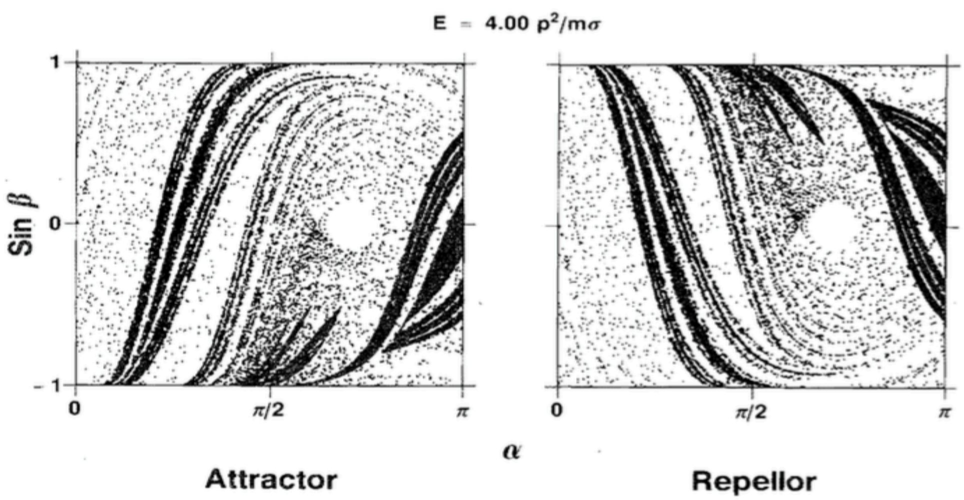


**Hoover, Physical Review A 37,** 252-257 **( 1 January 1988 )**

## The Reversibility of the Equations of Motion Implies the Presence of Attractor + Repellor Pairs of Fractal Objects

Nonequilibrium Systems driven by Time-Reversible motion equations produce symmetric phase-space flows from a MultiFractal Zero-Volume Repellor to a Mirror-Image attractor . The mirror image corresponds to time reversal . Zero phase volume explains the rarity of nonequilibrium stationary states . In addition, the repellors have a positive Lyapunov exponent sum corresponding to mechanical instability and unobservability . These features are fully consistent with the Second Law of Thermodynamics .

## Summary of the Situation in 1987-1990

Gauss' Principle of Least Constraint and Nosé-Hoover mechanics made it possible to simulate stationary nonequilibrium flows for systems of 100 or so particles with 4N or 6N equations of motion in two or three space dimensions . Although the equations were always time-reversible the results *never* were . Inevitably motion collapses onto a "strange attractor". The dimensionality of the attractor lies between the number of exponents in the last sum greater than zero and the first negative sum . Evidently the phase-space distribution is ( multi ) fractal and with zero volume relative to the equilibrium phase space. ( to be continued . . . )

## 6. An updated version of the Baker Map

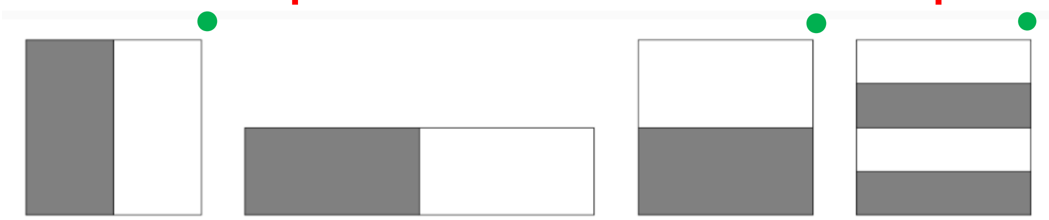

The Baker Map's mixing mechanism resembles that of a Baker kneading bread dough . First , stretch in the x direction . Second , make a central vertical cut . Third , replace the right half atop the left . This three-step process introduces new information in the x direction while aiscarding information in the y direction . As a result , a computer simulation of the Baker Map is doomed to fail after a few dozen iterations , converging to the fixed point at the upper righthand corner of the mapped area .

Because of our interest in time reversibility we consider here a rotated Baker Map ( suggested by Bill Vance ] . Not only does this modification introduce reversibility , so that TBT = $B^{-1}$ , it is also is a permanent source of "noise" due to the square roots which are a consequence of the rotation operation . This uptodate Baker Map is a great analog of nonequilibrium mechanics .

## 7. An updated version of the Baker Map

Information gleaned from an old model , the Baker Map , which was brought up-to-date by [ 1 ] a 45° rotation and [ 2 ] a provision for phase-space area change , corresponding to dissipation . The use of maps , rather than flows , means that chaos can be seen in just *Two* phase-space dimensions , not just the *Three* required for flows .

# An Updated Version of the Baker Map including the 45-degree rotation

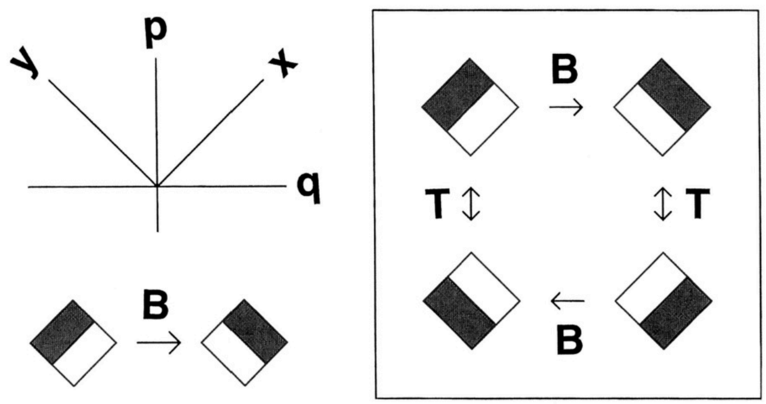


## Understanding the Source of Irreversibility through the Baker Map [ at and away from "equilibrium" and with single-precision arithmetic ] This is the "equilibrium" case which preserves area in the mapping .

Notice ! Single precision throughout !

```
if(q.lt.p) then
   qnew = +1.25*q - 0.75*p + sqrt(1.125)
   pnew = -0.75*q + 1.25*p - sqrt(0.125)
endif

if(q.gt.p) then
   qnew = +1.25*q - 0.75*p - sqrt(1.125)
   pnew = -0.75*q + 1.25*p + sqrt(0.125)
endif
```

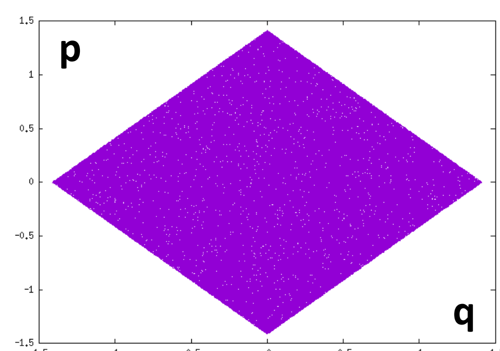


The plot is composed of 500 000 points ( gnuplot dots ) starting with ( qp ) = ( 0.6,0.8 ) .
The dots are part of the *transient* portion leading to a *periodic* orbit with 15 920 382 .

## 7. Understanding the Source of Irreversibility Through the Baker Map

Suppose we solve the equilibrium Baker Map starting at (0.6,0.8) with single precision .
I noticed that the ( coordinate,momentum ) pairs repeat every 15 920 382 iterations . *
The next idea was to generate a [ time-reversed ] trajectory starting with (0.6,-0.8) .
A search reveals that the q coordinates from the two initial conditions don't match .
A factorization shows that 15 920 382 = 2 x 3 x 41 x 64 717 which is mysterious !
Starting with (0.3,-0.4) again provides 15 920 382 [ again ] but (0.3,0.4) → 3 367 578 !

Although the initial parts of the mappings differ ( they are transients ) the final periodic orbits are mirror images of one another and the "equations of motion" are indeed unchanged if one changes the signs of both q and p .

Although the 15 920 382 points are too many to plot we can look at 0.01% of them after the transients have disappeared. We find that the two orbits are congruent !

* Motivated by Dellago and Hoover's rediscovery and investigations of a nice Periodic orbit paper : Grebogi, Ott, and Yorke, Physical Review A 38, 3688 (1988) .

I am curious whether or not C generates the same periodic orbit as FORTRAN .

## 7. Understanding the Source of Irreversibility Through the Baker Map

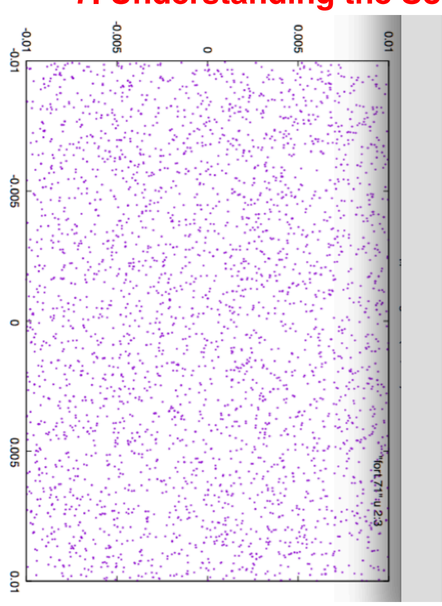


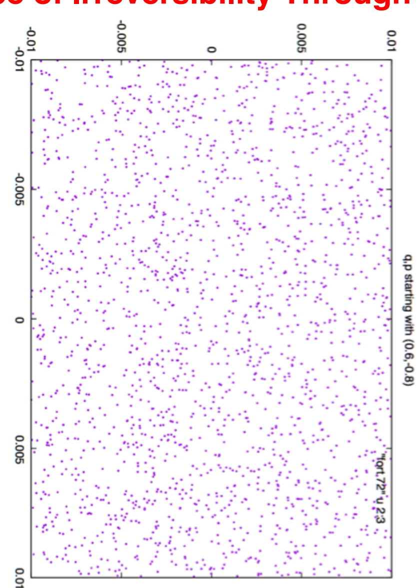


There is no apparent symmetry between the centered plots of width 0.02 and height 0.02 .

Looking at the tops or bottoms of the two plots revealed a similar lack of any symmetry .

Why are the periods Identical ?

## Understanding the Source of Irreversibility Through the Baker Map

Suppose we solve the equilibrium Baker Map starting at (0.6,0.8) with single precision .
We notice that the (coordinate,momentum) pairs repeat every 15 920 382 iterations :

| | | |
|---|---|---|
| 0.258040428 | -0.376516074 | 17414024 |
| 0.258040428 | 1.02718401 | 17441609 |
| 0.258040428 | 0.689610183 | 19365593 |
| 0.258040428 | -0.376516074 | 33334406 |
| 0.258040428 | 1.02718401 | 33361991 |
| 0.258040428 | 0.689610183 | 35285975 |
| 0.258040428 | -0.376516074 | 49254788 |

← (q,p) and iteration

Suppose we start at (0.6,-0.8) instead . Then we see :

| | | |
|---|---|---|
| 7.05265850E-02 | -0.822517037 | 9952250 |
| 7.05265850E-02 | -0.822517037 | 25872632 |
| 7.05265850E-02 | -0.822517037 | 41793014 |

Again notice the (coordinate,momentum) pairs repeat every 15 920 382 iterations :

A search reveals that the q coordinates from the two initial conditions don't match .

## 7. Understanding the Source of Irreversibility through the Baker Map : Even at Equilibrium we see the analogs of repellor/attractor pairs . All of the details of the 15 920 382 periodic-orbit points are present .

Note the inverted (q,p) scales

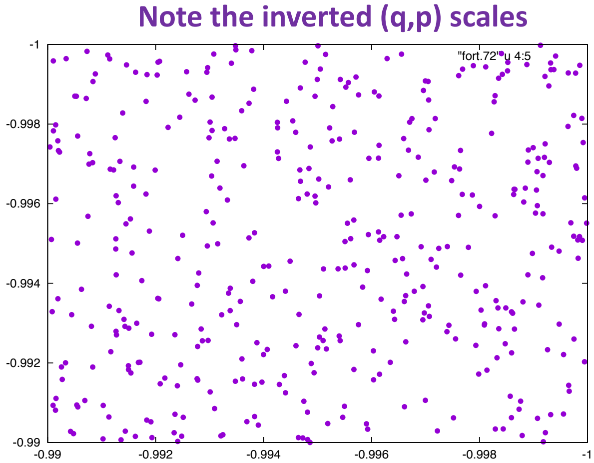


These plots are identical !

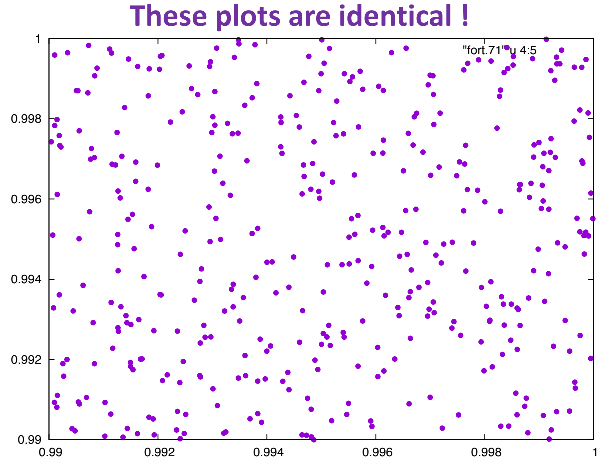

Understanding the Source of Irreversibility Through the Baker Map

Even *at* Equilibrium we see the analogs of repellor/attractor pairs .

All of the details of the 15 920 382 periodic-orbit points are present .

At equilibrium there are two mirror-image periodic orbits . They have identical lengths roughly equal to the square root of the number of state points . This is what we would "expect" from the Birthday Problem .

Let's look at the much simpler problem of a Nonequilibrium Steady State , where a portion of the map (2/3) undergoes compression independently of the direction of time .

## N people are in the room . Are their Birthdays different ?

**Probability that Second person's birthday is different = ( 1 – 1/ 365)**

**Second and Third = ( 1 – 1/365) ( 1 – 2/365) . . . [ integrate the log ]**

**$N^2/(2 \times 365) = ½ \rightarrow N = \sqrt{365} = 19$**

**An exacting calculation shows that 23 is the first probability to exceed ½ . In our Baker Map example the number of states is around $10^{16}$ . Let's consider the Nonequilibrium Baker Map next .**

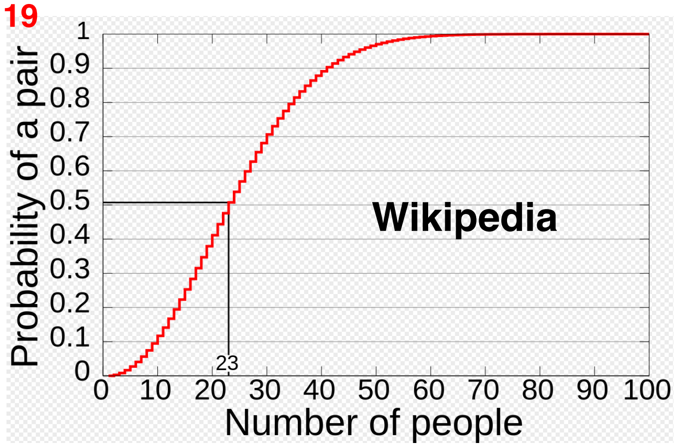

## 7. *Time Reversibility* of the Nonequilibrium Baker Map

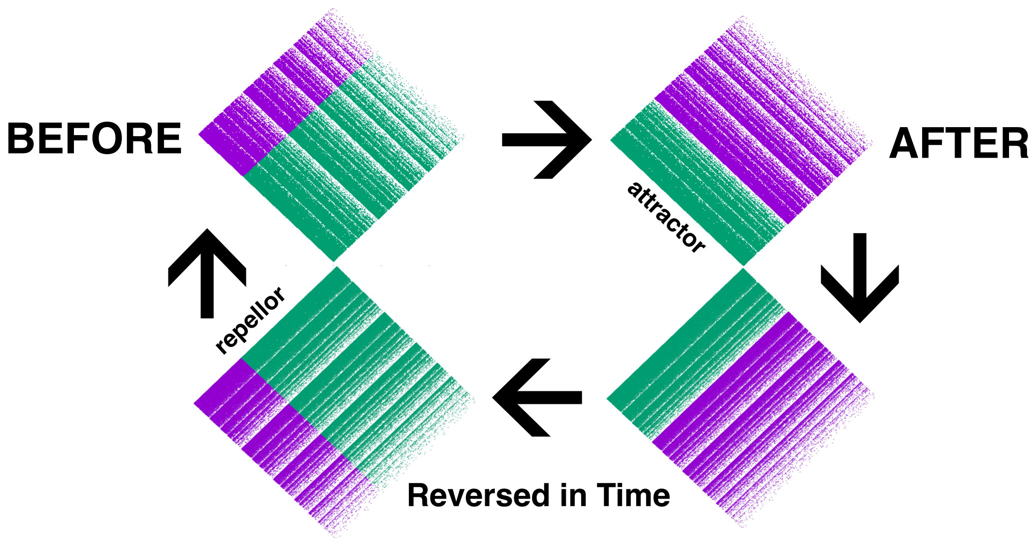


ANY TRANSFORMATION THAT IS ERGODIC HAS *SOME* COMPRESSION AND EXPANSION .
MOST OF THE MAP CORRESPONDS TO COMPRESSION GIVING A STRANGE ATTRACTOR .

## Past → Present → Future

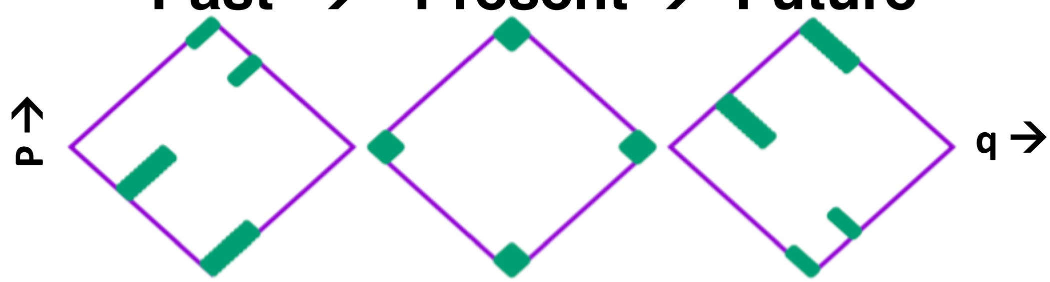


The strains for the upper two regions are ( 3 ; 2/3 ) and for the lower ( 3/2 ; 1/3 ) . These strains correspond to area changes of 2 at the top and 1/2 at the bottom .

The time-reversed version of the Baker Map B is TBT , where T changes ( q,p ) → ( q,-p ) .

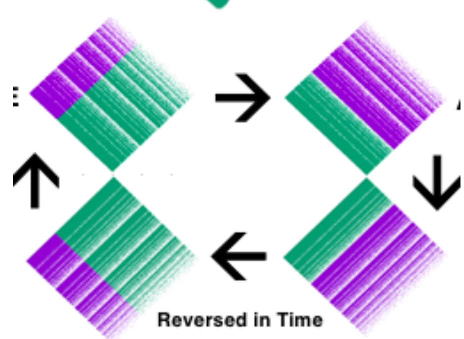

## Lyapunov Exponent Calculation for the Baker Map

**2/3 of the measure ( upper row ) expands by 3/2 while 1/3 of the measure expands three fold so that $\lambda_1 = (2/3)\ln(3/2) + (1/3)\ln 3 = 0.63651$ . The smaller Lyapunov exponent is $(2/3)\ln(1/3) + (1/3)\ln(2/3) =$ $-0.86756$ . The sum should be $-(1/3)\ln(2) = -0.23105$ and is ! Compression/Expansion = 2 for a mean value of $2^{1/3}$ .**

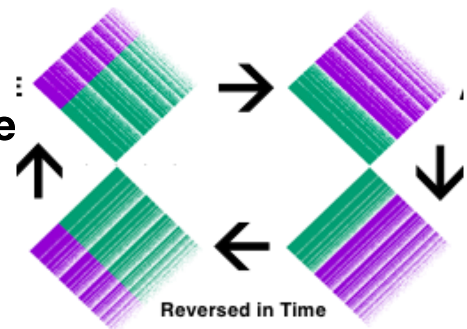


## 7. *Time Reversibility* of the Nonequilibrium Baker Map

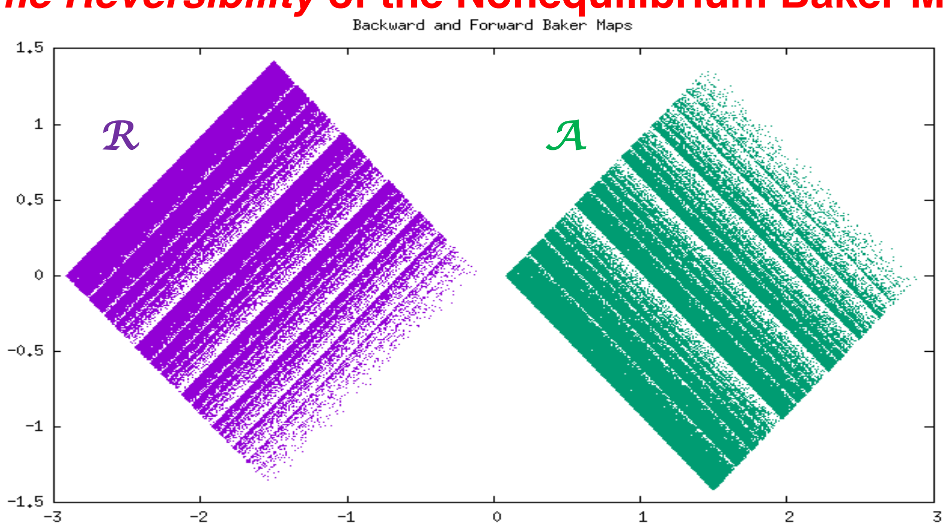


**BAKER MAP REPELLOR** **BAKER MAP ATTRACTOR**

**[ Reversed in Time by using the Reversed Map : $\mathcal{R} = \mathcal{TAT}$ ]**

# 7. *Time Reversibility* of the Nonequilibrium Baker Map

```
      do 60 it = 1,500 000
      if(q+p.lt.-dsqrt(2.0d00/9.0d00)) then
      qp = 11*q/6.0d00 + 7*p/6.0d00 + dsqrt(49.0d00/18.0d00)
      pp = 11*p/6.0d00 + 7*q/6.0d00 + dsqrt(25.0d00/18.0d00)
      endif
      if(q+p.gt.-dsqrt(2.0d00/9.0d00)) then
      qp = 11*q/12.0d00 + 7*p/12.0d00 - dsqrt(49.0d00/72.0d00)
      pp = 11*p/12.0d00 + 7*q/12.0d00 + dsqrt( 1.0d00/72.0d00)
      endif
      q = qp
      p = pp
      write(100,*) q,p
60    continue
```

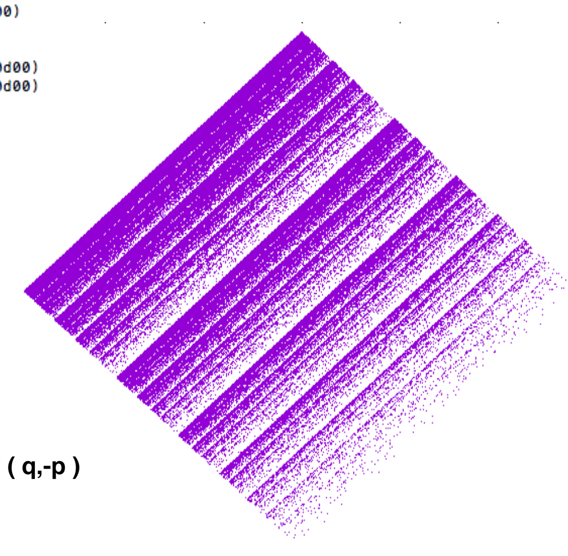

The repellor is no more difficult to construct than was the attractor . This FORTRAN program used the original Baker mapping with ( q,p ) replaced everywhere by ( q,-p )

# 7 . *Time Reversibility* of the Nonequilibrium Baker Map

One might well expect that the TBT mapping , because it can easily be checked to confirm that it returns to the previous ( q,p ) point , would generate the *same* attractor as was obtained by the forward mapping .

What happens is "something completely different" . Because reversing would be expected to preserve the attractor it is suprising to see instead a Repellor , with velocities *opposite* to those of the Attractor . Reversing would imply expansion of area , which is impossible in a bounded space .

Overall this is exactly the same experience that one would see with an irreversible movie . After seeing many "frames" , half a million in the Baker case , that all follow the same pattern , the time symmetry is broken and the highly-unlikely Lyapunov-unstable Repellor states are generated instead. The Baker Map is a good analog of the same reversibility lessons that we can learn from continuous particle flows .

## 7 . *Time Reversibility* of Nonequilibrium Steady States

**The Baker Maps nicely illustrate that the competition between expansion and compression is necessarily won by compression . Although any history that we generate simply follows a moving point, which can't change area, a collection of these points , as described by the Liouville Theorem can *never* expand in a steady state . Liouville requires compression, which is why we invariably observe fractal strange attractors in nonequilibrium steady states . Although this lesson is most easily seen for simple maps it is evident that the *same* mechanism,**

**Changing Phase Volume → Irreversibility and Strange Attractors**

**is also seen in the manybody systems to which molecular dynamics can be applied .**

**A second lesson , from the $\phi^4$ model , is that dimensionality loss is not limited to the phase-space coordinates which are thermostated . Because the phase-space offset vectors ( satellite minus reference ) *rotate* much more rapidly than they grow or decay it is feasible to see an overall dimensionality loss which greatly exceeds the number of thermostated pairs of phase-space coordinates . Our simple few-body models lead to an understanding of many-body ones and to an understanding of thermodynamic irreversibility . We discuss the $\phi^4$ model in the next lecture .**